

Soil Liquefaction due to Long Duration Earthquakes with Low Acceleration



J. Izawa & Y. Murono

Earthquake and Structural Engineering, Structures Technology Division, Railway Technical Research Institute

K. Tanoue

JR Central Consultants Company

SUMMARY:

Severe soil liquefaction due to a long duration earthquake with low acceleration occurred at Tokyo Bay area in the 2011 off the Pacific coast of Tohoku Earthquake. This phenomenon clearly shows that soil liquefaction is affected by properties of input waves. This paper describes effect of wave properties of earthquake on liquefaction using effective stress analysis with some earthquakes. Analytical result showed that almost the same pore water pressure was observed due to both a long duration earthquake with max acceleration of 150 gal and typical inland active fault earthquake with 891gal. Additionally, liquefaction potentials for each earthquake were evaluated by assessment of liquefaction potential with accumulated damage, which is used for design of railway structures in Japan. As a result, it was found that accurate liquefaction resistance on large cyclic area is necessary to evaluate liquefaction potential due to a long duration earthquake with low acceleration by assessment of liquefaction potential with accumulated damage.

Keywords: Liquefaction, Long duration earthquake, Liquefaction strength curve, Effective stress analysis

1. INTRODUCTION

Liquefaction of saturated cohesion less soil was observed in the past severe earthquakes in Japan, such as 1995 Hyogo-ken Nambu earthquake, 1964 Niigata earthquake and so on. Such liquefaction areas were located near the epicentre of each earthquake, and are considered to have been heavily vibrated by strong earthquake motion. On the other hand, in the 2011 off the Pacific coast of Tohoku Earthquake, severe liquefaction was observed at Tokyo Bay area, where is far from the epicentre and observed acceleration was less than 200 Gal. The main reason for such liquefaction due to low acceleration earthquake is considered to be very long shaking duration, which was longer than 300 seconds. Thus, effect of characteristics of input earthquakes on soil liquefaction should be properly evaluated in design.

Liquefaction potential is generally assessed by FL method. FL method determines factor of safety by comparing the shear stress ratio acting on the soil layer, L and the liquefaction resistance, R . In many case, R_{20} is used as the liquefaction resistance. R_{20} is the shear stress ratio that needs cyclic number of 20 to make a soil layer liquefied. Specification for Highway Bridges (Japan Railway Association) uses correction factor on irregularity of input earthquake, C_w which can increase R_{20} against earthquakes with large acceleration and short duration, such as near field earthquake. On the contrary, C_w is 1.0 for ocean trench earthquake. These values were obtained from assessment of liquefaction potential with accumulated damage (D value) with liquefaction resistance curve of Toyoura sand (Higashi et al.). In Design standard for railway structures, effect of characteristics of input earthquakes on soil liquefaction resistance is directly considered by using accumulated damage on each liquefaction layer and design earthquake. However, applicability of the method has not been verified for long duration earthquakes with low acceleration. This paper describes the effect of characteristics of input earthquakes on soil liquefaction. At first, effective stress analyses are conducted with some earthquakes including a long duration earthquake with low acceleration. Furthermore, assessments on liquefaction potential with accumulated damage against the same input earthquakes used in the effective stress analyses are conducted, and results are compared with results of effective stress analyses.

2. INPUT EARTHQUAKES

4 types of input waves, Kobe A, Kobe B, Tomakomai and Urayasu wave were used in effective stress analyses and assessment of liquefaction potential, as shown in Figure 1. Kobe A was recorded at Kobe Japan Marine Association in 1995 Hyogo-ken Nambu earthquake, which was a typical near field earthquake, whose maximum acceleration, A_{max} is 818.8 Gal. Table 1 listed maximum acceleration, A_{max} and Acceleration power, I_E of each input wave. I_E can be calculated by the following equation.

$$I_E = \int_0^T a^2 dt \quad (1)$$

where, a is acceleration (Gal) and T is the duration of earthquake(sec.). A_{max} of Kobe B is corrected to have the same maximum acceleration of Urayasu wave, whose maximum acceleration is 156.6 Gal. Both A_{max} and I_E of Kobe B are about 20% of those of Kobe A as shown in Table 1. Tomakomai wave is based on the time history recorded at K-NET Tomakomai in 2003 Tokachi-oki earthquake. A_{max} of Tomakomai wave is also corrected to be 156.6 Gal. Urayasu wave is the typical long duration and low acceleration earthquake observed in the 2011 off the Pacific coast of Tohoku Earthquake observed at Tokyo Bay area (K-NET Urayasu). As mentioned above, A_{max} of Urayasu wave is the same with Kobe B and Tomakomai, and about 20% of that of Kobe A. I_E of the Urayasu wave is almost the same with Tomakomai, too. As shown in Figure 1, duration of Tomakomai and Urayasu wave are longer than 300 seconds. On the other hand, Kobe A and B are about 20 seconds.

Figure 2 shows the Fourier spectrums of input waves. Natural frequencies of Urayasu wave and corrected Tomakomai wave are about 0.9 Hz and 0.3 Hz. It means that Tomakomai wave is a long duration and long period earthquake.

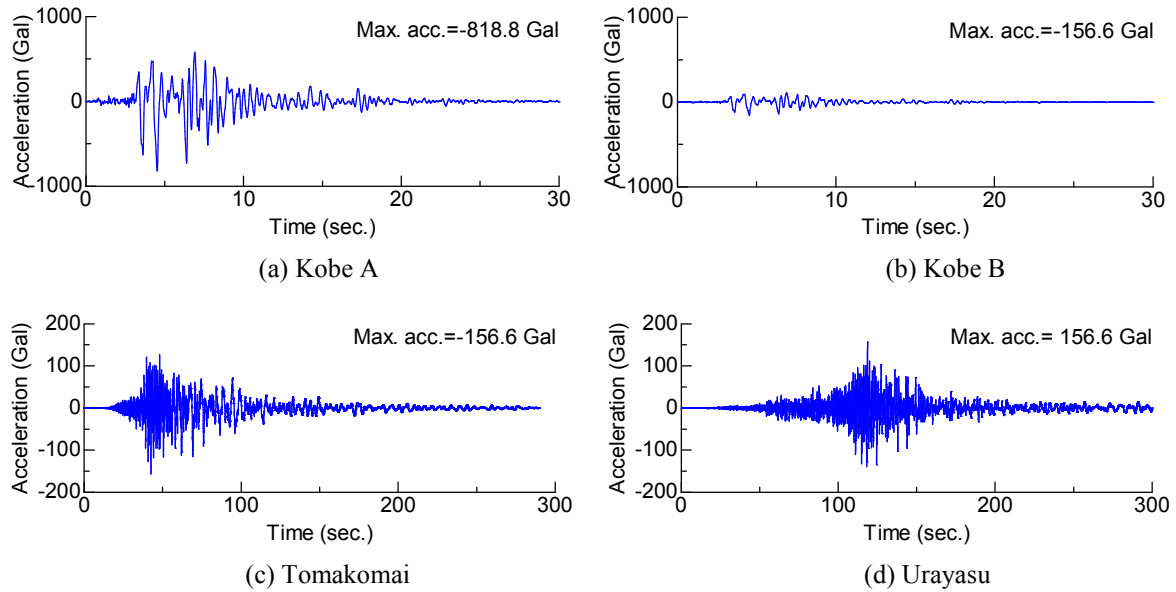


Figure 1 Input waves

Table 1 Properties of input waves

Waves	Max. acc.(Gal)	Acc. Power, $I_E(\text{cm}^3/\text{s}^2)$	Remarks
Kobe A	-818.8 (5.23)	525130 (5.10)	1995 Hyogo-ken Nambu EQ. (Kobe Japan Marine Association)
Kobe B	-156.6 (1.00)	19215 (0.19)	Max. acc. of Kobe A is corrected to be 156.6 Gal.
Tomakomai	-156.6 (1.00)	100260 (0.97)	2003 Tokachi-oki EQ. (K-NET Tomakomai) Max. acc. is corrected to be 156.6 Gal.
Urayasu	156.6 (1.00)	102964 (1.00)	2011 Tohoku Great EQ. (K-NET Urayasu)

※(): ratio of max. acc. and acc. power of each wave to those of Urayasu wave

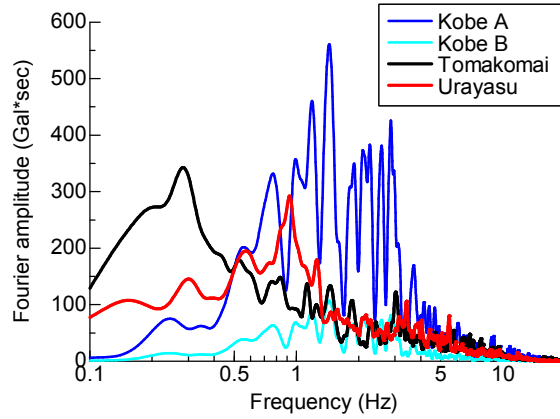


Figure 2 Fourier spectrums of input waves

3. EFFECTIVE STRESS ANALYSES

3.1. Outline of analyses

One dimensional effective stress analyses were carried out with Multi-Spring model (Towhata and Ishihara) and excess pore pressure model of Iai et al. *Fukaehama ground* was selected as the model ground, which is an Island reclaimed with Decomposed Granite soil near Kobe Port Island, where severe liquefaction was observed in 1995 Hyogo-ken Nambu Earthquake. Parameters for effective stress analysis are listed in Table 2 (Miwa et al.). Upper layer with depth of 14.8m is reclaimed with Decomposed Granite soil (DG layer). Ground water table is located at the depth of 3.8m, and DG layer 2~3 below the water table are considered to be liquefaction layer.

Table 2 Soil parameters for effective stress analyses (Miwa et al.)

	Depth (m)	γ (kN/m ³)	V_s (m/s)	ν	h_{max}	G_{m0} (kN/m ²)	K_{m0} (kN/m ²)	ϕ (°)	Liquefaction parameters					
									ϕ_p (°)	S_1	w_1	p_1	p_2	c_1
DG soil 1	3.8	20.6	100	0.435	0.24	21020	154780	30	-	-	-	-	-	-
DG soil 2	6.6	20.6	170	0.435	0.24	60749	447314	30	28	0.005	33.1	0.5	1.27	1.0
DG soil 3	9.5	20.6	160	0.443	0.24	53812	451939	30	28	0.005	33.1	0.5	1.27	1.0
DG soil 4	14.8	20.6	200	0.486	0.24	84082	2972146	30	28	0.005	26.0	0.5	1.22	1.5
Alluvial deposit	20.7	16.7	160	0.486	0.24	53812	1902173	30	-	-	-	-	-	-
	26.7	18.6	200	0.492	0.24	68041	4378001	30	-	-	-	-	-	-
Diluvial deposit	28.0	20.6	240	0.489	0.24	109558	4958575	30	-	-	-	-	-	-
	30.7	20.6	210	0.487	0.24	92700	3453182	30	-	-	-	-	-	-
	33.7	20.6	270	0.488	0.24	153239	6281284	30	-	-	-	-	-	-

* DG soil: Decomposed granite soil : Liquefaction layer

3.2. Results and Discussions

Figure 3 shows time histories of excess pore water pressure, $\Delta u/\sigma'_c$ surface acceleration and surface displacement of DG layer 2 and 4 for each input wave. When the ground was shaken with Kobe A wave, DG layer 2 and 4 showed $\Delta u/\sigma'_c$ of about 0.9. In general, if $\Delta u/\sigma'_c$ reaches about 0.95, it is considered that liquefaction occurs. Then, the DG layer 2 did not reach liquefaction although excess pore water pressure was very high. In the case Kobe B wave, $\Delta u/\sigma'_c$ in DG layer 2 reached about 0.5 even though acceleration amplitude of Kobe B is about 20% of that of Kobe A. On the other hand, $\Delta u/\sigma'_c$ in DG layer 4 was only about 0.2, probably because parameters are different from those of DG layer 2. This means that increase of pore water pressure against low acceleration earthquake may be sensitively influenced by characteristics of ground.

In the case of Tomakomai and Uraywasu wave, $\Delta u/\sigma'_c$ reached 0.95 in DG layer 2, which was higher than that of Kobe A case. This result clearly shows that liquefaction may occur due to long duration earthquake even though the acceleration is low. On the other hand, pore water pressure of DG layer 4

was very low in both cases. As mentioned in the case of Kobe B wave, DG layer 4 may have large liquefaction resistance against long duration earthquake with low acceleration. This layer had the value of c_1 1.5 times as large as that of DG layer 2 or 3 as shown in Table 2, which was determined by fitting the liquefaction strength curve obtained from liquefaction strength tests of each DG layer (Miwa et al.). The c_1 is the parameter that controls the effect of elastic shear work on increase of excess pore water pressure. That is, increase of excess pore water pressure due to low acceleration can be prevented by large c_1 value because most of all the shear work is dominated by elastic shear work if acceleration is low. Therefore, it is considered that excess pore water pressure did not increase in DG layer 4 in the case of Kobe B, Tomakomai and Urayasu wave.

After liquefaction occurs or pore water pressure increases to some extent, shear wave cannot pass through the ground since stiffness of the ground is very low. On the other hand, ground displacement may show large amplification. Such phenomena can be seen in all the cases after liquefaction occurred as shown in Figure 3. Especially in Tomakomai case, very large displacement can be seen in the time period from 70 to 80 seconds. In this case, horizontal displacement of the liquefaction layer with low stiffness may be amplified by long period input wave, which can be seen in the latter half of input wave, because the natural period of the ground increased. On the other hand, such large amplification of displacement was not observed in Urayasu case because Urayasu wave does not have long period composition, as shown in Figure 2.

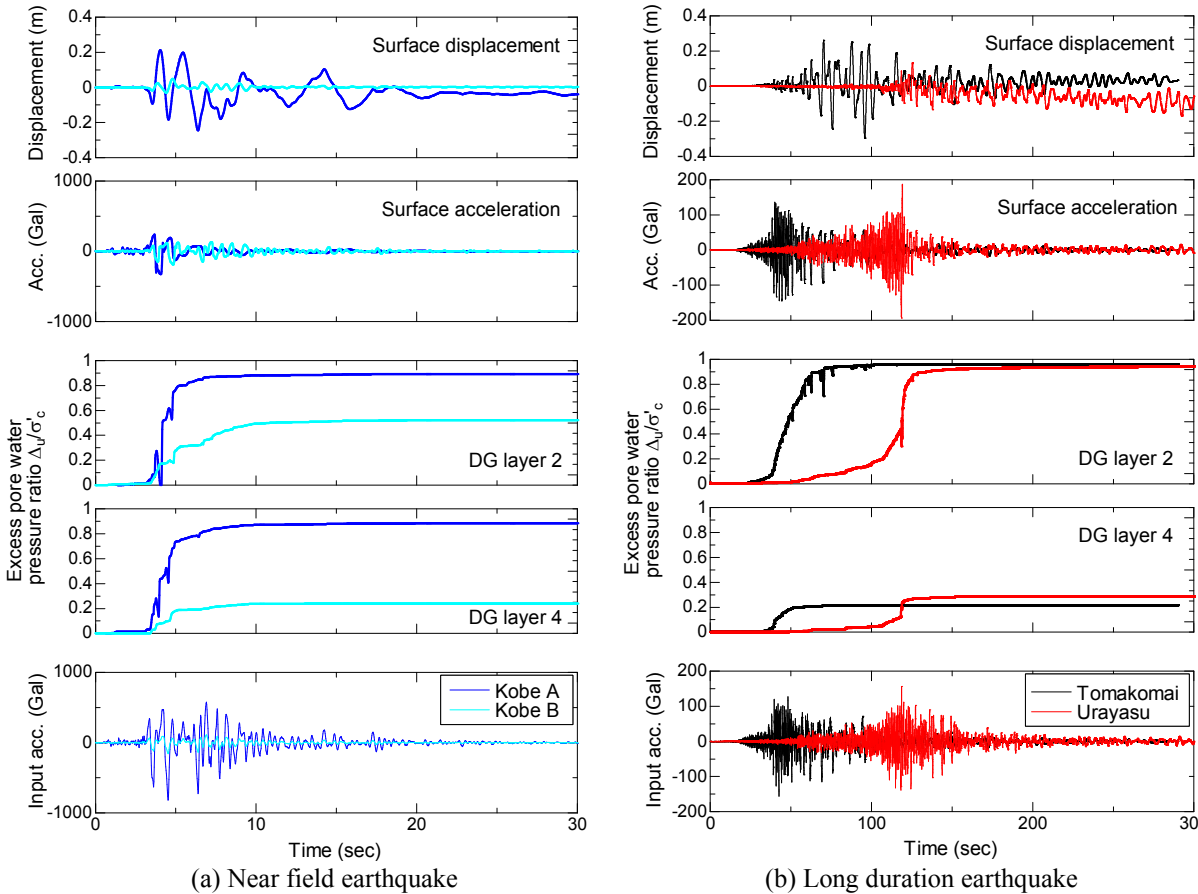


Figure 3 Time histories of excess pore water pressure, surface acceleration and surface displacement

4. ASSESSMENT OF LIQUEFACTION POTENTIAL

4.1. Assessment with accumulated damage (D value)

Results of effective stress analyses revealed that liquefaction may occur if duration of earthquake is sufficiently long, even though its amplitude is small. In this section, we will discuss applicability of

usual method to assessment of liquefaction potential. As mentioned in the introduction, liquefaction potential is assessed by FL method based on the accumulated damage (D value) theory in the Japanese railway standard, which can take into consideration the effect of irregularity of input earthquakes. Procedure of the method is as follows.

Firstly, a liquefaction resistance for cyclic number of 20, R_{20} is determined from laboratory tests or estimated with N value indicated in the railway standard. Then, the liquefaction resistance curve, which shows the relationship between liquefaction resistance, R_i and number of cycles, N_c can be estimated by the following equation (2), where relative density, Dr is also estimated from N value.

$$\left\{ \begin{array}{l} \text{i) } N_c \leq 20 \quad R_i = R_{20} \left(\frac{N_c}{20} \right)^{-1.35 \exp(-3.64 + 0.037 Dr)} \\ \text{ii) } N_c > 20 \quad R_i = R_{20} \left(\frac{N_c}{20} \right)^{-0.23} \end{array} \right. \quad (2)$$

Secondly, peak accelerations of ground surface are picked up with zero crossing method and peak values of shear stress acting on soil layers are calculated by the following equations.

$$L = (1.0 - 0.015z) \frac{a \sigma'_v}{g \sigma_v} \quad \text{for a near field earthquake} \quad (3)$$

$$L = (1.0 - 0.005z) \frac{a \sigma'_v}{g \sigma_v} \quad \text{for an ocean trench earthquake} \quad (4)$$

where L : peak shear stress ratio, z : depth of ground(m), a : surface peak acceleration(Gal), g : gravity(Gal), σ_v : total vertical stress(kN/m²), σ'_v : effective vertical stress(kN/m²). The largest peak shear stress ratio, L_{max} is used as seismic load in the assessment.

Necessary cyclic number that can make a soil layer liquefied with each peak shear stress can be obtained from the liquefaction strength curve. Then, accumulated damage, D can be calculated by the equation (5).

$$D = \sum \frac{1}{2N_c} \quad (5)$$

When the accumulated damage, D reaches 1.0, it can be assessed that liquefaction occurs. Then, peak shear stress ratio is repeatedly corrected until D becomes just 1.0. When D is equal to 1.0, the largest peak shear stress ratio, L'_{max} is set to be R_D , which is the liquefaction resistance corrected with accumulated damage. Finally, the liquefaction resistance, R_L which is corrected in consideration of stress anisotropy in natural ground, is determined by the equation (6).

$$R_L = \frac{1 + 2K_0}{3} R_D \quad (6)$$

Liquefaction potential can be assessed with the following equation.

$$F_L = \frac{R_L}{L_{max}} \quad (7)$$

If the $F_L < 1.0$, the ground is assessed as liquefaction ground. Degree of liquefaction of the ground can be evaluated with P_L value obtained by the following equation.

$$P_L = \int_0^H (1 - F_L)(10 - 0.5z) dz \quad (8)$$

where H : length of liquefaction layer (m), z : depth(m), and z is less than 20m. If $P_L > 5$, the ground is assessed as liquefaction ground. If $P_L > 20$, severe liquefaction may occur.

4.2. Results of assessment

Table 3 shows results of assessment of liquefaction potential with accumulated damage for each input wave. In the case of Kobe A wave, F_{LS} of all three DG layers 2~4 indicate the values lower than 1.0 and P_L is equal to 44.0, that is, this ground is assessed as severe liquefaction ground for Kobe A wave.

On the other hand, in the case of Tomakomai and Urayasu wave, which are long duration earthquakes with low acceleration, F_{LS} of DG layer 2 and 3 are less than 1.0, but P_{LS} are about 2.0. This ground is assessed as non liquefaction ground for the Tomakomai and Urayasu waves. The results of effective stress analyses clearly show that severe liquefaction occurred due to both Urayasu and Tomakomai waves. This discrepancy means that assessment of liquefaction potential with accumulated damage cannot evaluate liquefaction potential for long duration earthquake with low acceleration, under the assumption that the effective stress analysis can simulate actual ground behaviour. However, this discrepancy is attributed to the difference between liquefaction resistance curves used in effective stress analysis and assessment. The curves for assessment are determined from N value and the equation (1). On the other hand, the curves for effective stress analysis were determined by fitting the liquefaction strength curve obtained from liquefaction strength tests. Therefore, assessments are conducted with the liquefaction resistance curves, which were used in the effective stress analyses. Results are listed in Table 4. P_{LS} for Urayasu wave and Tomakomai wave are about 16, that is, the ground can be assessed as liquefaction ground. However, difference between P_{LS} of Kobe wave and those of Urayasu and Tomakomai waves is still large.

To investigate the reason for such large discrepancy between assessments and effective stress analyses, shear stress acting on the layer will be focused on. Time histories of excess pore water pressure ratio, $\Delta u/\sigma'_c$ obtained from effective stress analyses, cumulative damage parameter, D obtained from assessment, shear stress ratio obtained from both effective stress analyses and assessment, are indicated in Figure 6. The accumulated damage parameter, D is considered to be a factor, which is associated with excess pore water pressure ratio, $\Delta u/\sigma'_c$. In the case of Urayasu, Tomakomai and Kobe B wave, which are low acceleration waves, shear stress ratios used in assessment are relatively similar to those used in effective stress analyses. In addition, accumulated damage parameter, D shows also good agreement with $\Delta u/\sigma'_c$.

Table 3 Result of Liquefaction Judgment

(a) Kobe A							(b) Kobe B						
	R_{20}	R_L	R_L/R_{20}	L	F_L	ΔP_L		R_{20}	R_L	R_L/R_{20}	L	F_L	ΔP_L
DG layer 2	0.25	0.386	1.54	1.580	0.244	15.4	DG layer 2	0.25	0.386	1.54	0.302	1.28	0.00
DG layer 3	0.24	0.382	1.59	1.557	0.245	13.3	DG layer 3	0.24	0.382	1.59	0.298	1.28	0.00
DG layer 4	0.25	0.408	1.63	1.524	0.267	15.2	DG layer 4	0.25	0.408	1.63	0.291	1.40	0.00
					$P_L=$	44.0						$P_L=$	0.00
(c) Tomakomai							(d) Urayasu						
	R_{20}	R_L	R_L/R_{20}	L	F_L	ΔP_L		R_{20}	R_L	R_L/R_{20}	L	F_L	ΔP_L
DG layer 2	0.25	0.267	1.07	0.286	0.934	1.34	DG layer 2	0.25	0.269	1.08	0.286	0.940	1.22
DG layer 3	0.24	0.261	1.09	0.273	0.957	0.762	DG layer 3	0.24	0.263	1.10	0.273	0.962	0.663
DG layer 4	0.25	0.268	1.07	0.254	1.057	0.000	DG layer 4	0.25	0.270	1.08	0.254	1.06	0.00
					$P_L=$	2.10						$P_L=$	1.88

Table 4 Result of Liquefaction Judgment

(a) Kobe A							(b) Kobe B						
	R_{20}	R_L	R_L/R_{20}	L	F_L	ΔP_L		R_{20}	R_L	R_L/R_{20}	L	F_L	ΔP_L
DG layer 2	0.19	0.261	1.37	1.580	0.165	17.0	DG layer 2	0.19	0.261	1.37	0.302	0.863	2.80
DG layer 3	0.19	0.259	1.36	1.557	0.166	14.7	DG layer 3	0.19	0.259	1.36	0.298	0.871	2.28
DG layer 4	0.20	0.258	1.29	1.524	0.169	17.3	DG layer 4	0.20	0.258	1.29	0.291	0.887	2.36
					$P_L=$	49.0						$P_L=$	7.44
(c) Tomakomai							(d) Urayasu						
	R_{20}	R_L	R_L/R_{20}	L	F_L	ΔP_L		R_{20}	R_L	R_L/R_{20}	L	F_L	ΔP_L
DG layer 2	0.19	0.191	1.01	0.286	0.667	6.79	DG layer 2	0.19	0.189	0.995	0.286	0.660	6.92
DG layer 3	0.19	0.192	1.01	0.273	0.703	5.25	DG layer 3	0.19	0.190	1.000	0.273	0.697	5.36
DG layer 4	0.20	0.203	1.01	0.254	0.802	4.12	DG layer 4	0.20	0.203	1.015	0.254	0.800	4.16
					$P_L=$	16.2						$P_L=$	16.4

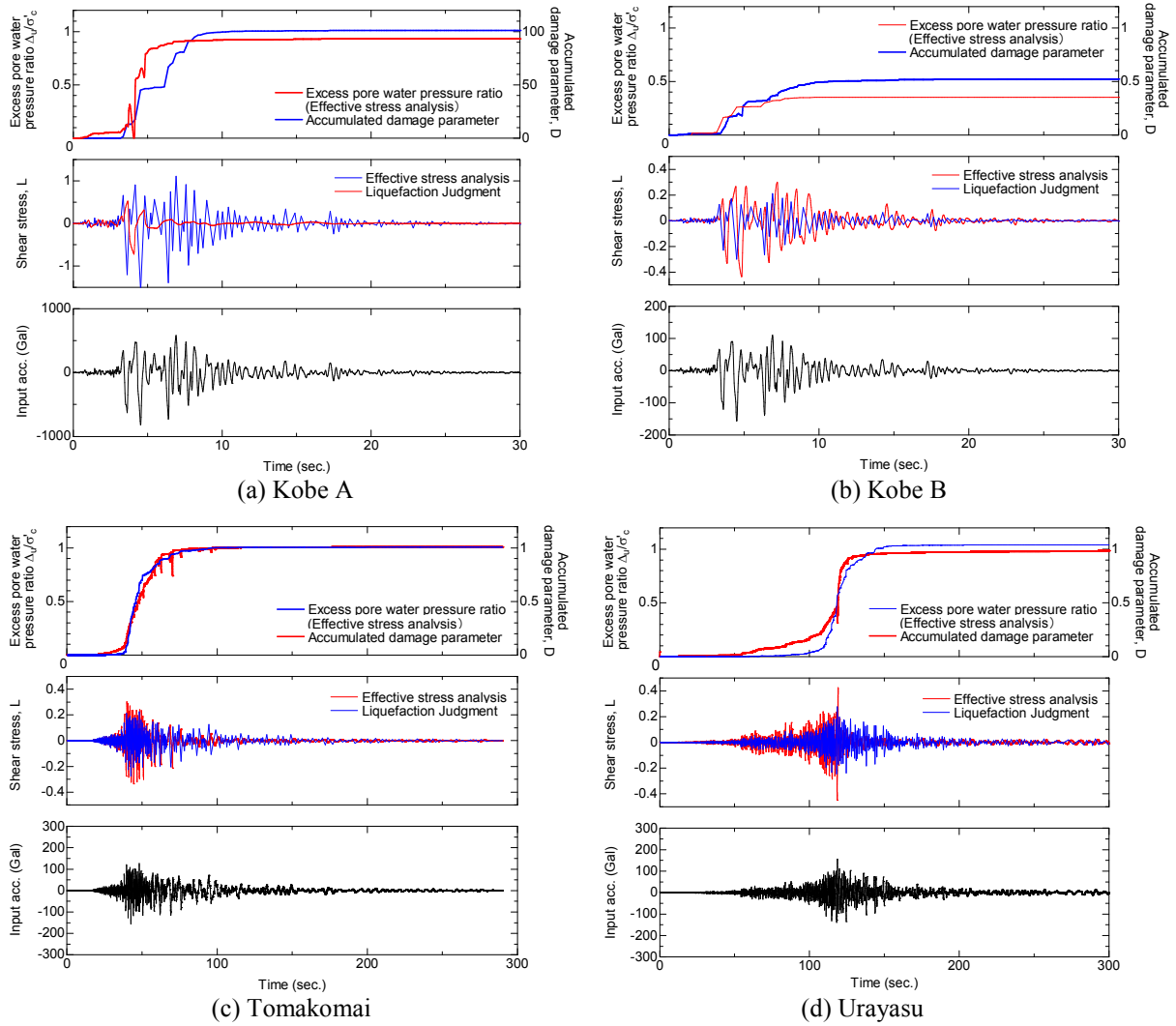


Figure 6 Comparison between Effective stress analyses and Liquefaction Judgments

On the other hand, in the case of Kobe A wave, large discrepancy is seen in shear stress ratio. The result of effective stress analysis shows rapid decrease of shear stress ratio after about 8 seconds because of low ground stiffness due to liquefaction. On the other hand, in the assessment, such tendency cannot be simulated because decrease of ground stiffness due to liquefaction was not considered. It is considered that over estimation of shear stress ratio in the assessment leads to large P_L for Kobe A wave. However, trend of increase of pore water pressure obtained from effective stress analyses can be relatively simulated by accumulated damage parameter, D . Consequently, for an earthquake with large acceleration, although occurrence of liquefaction potential can be assessed, there is possibility of over estimation of shear stress ratio for earthquakes with large acceleration.

5. CONCLUSIONS

This paper describes the effect of characteristics of input earthquakes on soil liquefaction. At first, effective stress analyses were conducted with some earthquakes including a long duration earthquake with low acceleration. Furthermore, assessments of liquefaction potential with accumulated damage for the same input earthquakes were conducted and results were compared with results of effective stress analyses. As a result, the following conclusions are obtained.

- (1) Results of effective stress analyses revealed that liquefaction may occur if duration of earthquake

is longer, even though its amplitude is small.

- (2) Assessment of liquefaction potential with accumulated damage can simulate trend of increase of pore water pressure in ground. However, there is possibility of over estimation of shear stress ratio for earthquakes with large acceleration because decrease of ground stiffness due to liquefaction is not considered.

ACKNOWLEDGEMENT

The K-NET records used in this paper were observed by the National Research Institute for Earth Science and Disaster Prevention.

REFERENCES

- Japan Road Association. (2002). *Specification for Highway Bridges*, Tokyo Japan. (in Japanese)
- Azuma, T., and Tamura, K. (1997). Estimation of the Liquefaction Strength Considering Ground motion Characteristics, *Doboku Gijutu Siryo*, **Vol. 39-9**, pp. 50-55. (in Japanese)
- Railway Technical Research Institute. (1999). *The Design Standards for Railway Structures and Commentary (Seismic Design)*, Supervised by Ministry of Land, Infrastructure and Transportaion, Maruzen. (in Japanese)
- Towhata, I. and Ishihara, K. (1985). Modeling soil behavior under principal stress axes rotation, *Proc. of 5th International Conf. on Num. Methods in Geomechanics*, **Vol.1**, pp. 523-530.
- Iai, S. Matsunaga, M. and Kameoka, T. (1992). Strain Space Plasticity Model for Cyclic Mobility, *Soils and Foundations*, **Vol. 32, No. 2**, pp. 1-15.